Hindawi
Advances in Materials Science and Engineering
Volume 2022, Article ID 6110591, 11 pages
https://doi.org/10.1155/2022/6110591

Research Article

Optimization of Abrasive Wear Characteristics of Polyethylene/Acrylate Copolymer Nanocomposites

S. Chockalingam,[1] G. Gopalarama Subramaniyan,[2] Anand Bisen,[3] S. Kaliappan,[4] S. Sekar,[5] Pravin P. Patil,[6] T. Ch. Anil Kumar,[7] B. Ramesh,[8] and S. Venkatesan[9]

[1]*Department of Mechanical Engineering, E.G.S. Pillay Engineering College, Nagapattinam, India*
[2]*Department of Mechanical Engineering, Saveetha Engineering College, Chennai, India*
[3]*Mechanical Engineering Department, Kalaniketan Polytechnic College Jabalpur (M.P.), Pin:482001, Jabalpur, India*
[4]*Department of Mechanical Engineering, Velammal Institute of Technology, Chennai 601204, Tamil Nadu, India*
[5]*Department of Mechanical Engineering, Rajalakshmi Engineering College, Rajalakshmi Nagar Thandalam, Chennai 602 105, Tamilnadu, India*
[6]*Department of Mechanical Engineering, Graphic Era Deemed to be University, Bell Road, Clement Town 248002, Dehradun, Uttarakhand, India*
[7]*Department of Mechanical Engineering, Vignan's Foundation for Science Technology and Research, Vadlamudi 522213, India*
[8]*Institute of Mechanical Engineering, Saveetha School of Engineering, Saveetha Institute of Medical and Technical Sciences, Chennai 602 105, Tamil Nadu, India*
[9]*School of Mechanical Engineering, College of Engineering and Technology, Wachemo University, Hosaena, Ethiopia*

Correspondence should be addressed to S. Venkatesan; profsvenkatesan@gmail.com

Received 7 April 2022; Accepted 7 June 2022; Published 27 June 2022

Academic Editor: Vijayananth Kavimani

Polymer nanocomposites are being used more widely in a variety of industries. As the compatibilizer, Elvaloy-AC-3427 (EAC) was used in addition to Cloisite 30B (C3B) as the reinforcement of filler in this research. For the production of Polyethylene/Cloisite 30B/Elvaloy AC-3427 nanomaterials, a twin-screw extruder is employed. Cloisite 30B was added to the Polyethylene matrix in the range of 2%, 3%, 4%, and 5%. The mechanical and thermal characteristics of the compounds have been examined. Nanocomposites were tested for their tribological properties utilizing abrasive wear load, C3B, and sliding distance which were all taken into consideration while performing the abrasive wear evaluations. Specific wear rate (SWR), coefficient of friction (COF), and weight loss were the abrasive wear test's output metrics (SWR). For the purpose of enhancing the abrasive wear characteristics, grey relational analysis and grey fuzzy were used. An ANOVA was carried out to examine the connection between input parameters and output variables. Finally, the Polyethylene/Cloisite 30B/Elvaloy AC-3427 nanocomposites abraded wear samples were evaluated microscopically.

1. Introduction

Researchers have been investigating Polyethylene-coated composite with supplements for the production of polymer nanoparticles for the last several decades. Additives are used to enhance several characteristics of the polymer matrix, including mechanical, thermal, and optical properties [1, 2]. Glass fibers, CNTs, nanoclays, and other traditional fillers can make up to 40% of the polymer matrix's weight, whereas nanotype fillers can make up to 5% of the weight. The manufacture of polymer nanocomposites may be made more cost-effectively by using fillers with low molecular weight [3]. Polymer nanocomposites may be made using a variety of ways, although the melt intercalation approach is the most common. To do melt intercalation, extruders (either single or twin) must be used [4]. Owing to the low

price, simplicity of processing, and availability in the marketplace, Polyethylene is the most commonly utilized substance [5]. For its better physical and thermal qualities, [6] determined that PE is the most frequently used substance. Even while PE has several advantages, its weak strength and poor stiffness render it inapplicable in most cases. Fillers such as mica and other fillers have been used in the PE to counteract its shortcomings. Additional abrasion resistance was needed to compensate for the higher strength and stiffness that fillers provided [5, 7]. According to earlier research, reinforcing nanoclays into the PE matrix is advantageous. Due to the hydrophobic nature of PE, it is difficult to spread nanoclays inside it. PE nanoclays were not well dispersed as a result of this occurrence [8]. Several writers have utilized various kinds of compatibilizers to circumvent this limitation [9, 10].

The study of polymer nanocomposites' tribological properties is essential for determining the materials' friction and wear. The pace of substance ejection may be sluggish, but it is a recurring one [11, 12]. Poly was the study's compatibilizer (ethylene co-glycidyl methacrylate) where load, abrading distance, and grit size were all considered input factors. The results showed that the inclusion of a compatibilizer increased abrasion resistance. An abrasive wear test that used worn surface morphology revealed microploughing as a wear process [13–15]. Because of this, they came to the conclusion that adding ZnO nano to ultrahigh molecular weight PE had a lower rate of wear than doing so in microform. According to microzno, the worn surface morphology shows that nanozinc oxide adds rather homogenous layers.

Grey Relational Analysis is a technique that uses black to represent a dearth of information and white to represent a surplus of data. There are a variety of descriptive terms for the region that is just outside of these two extremes [16]. There are sections of the system that are recognized, and there are parts of the system that do not have any information at all. GRA defines information quality and quantity as either finished or not yet finished, i.e., from black to white through the grey scale [17, 18]. When it comes to GRA, there is always a degree of ambiguity because of a wide range of possible data points. It is possible to go to the end of the GRA process with almost no information at all, and at the other end, there will be a unique answer. The optimal answer cannot be found by using GRA, but it may be used to identify a suitable solution [19, 20].

During the time of abrasive wear procedure, the input constraints of abrasive wear have a significant impact. Optimizing the input settings is essential to want better outcomes. These days, fuzzy logic, scatter search, and a host of other approaches are the most often utilized optimization methods. According to [21, 22], an optimization approach was developed to improve the multiple bead shape during submerged arc welding. For the optimization of various answers, the study in [23, 24] used a combined approach known as the Taguchi method and artificial intelligence.

GRA has been utilized in recent years to improve operations like welding, machining, and turning. When the fuzzy logic theory was applied to the GRA, it became even better. Research by [25–27] examined the drilling properties of CFRP compound plates. Optimizing the drilling experiment's result was done using GRA and grey fuzzy. Grey fuzzy's grade values were discovered to be higher than GRA's.

Despite the fact that a variety of other fillers have been used to strengthen the PE matrix, no one has reported on the usage of EAC as a compatibilizer [28–30]. Even though only limited research reports were available on the abrasive wear properties of the Polyethylene/Cloisite 30B/Elvaloy AC-3427 NCs, a twin-screw extruder was utilized to make the Polyethylene/Cloisite 30B/Elvaloy AC-3427 NCs which was used in this investigation. Cloisite 30B concentrations in the PE matrix were changed from 1% to 5%. They were made using the injection molding method. The tests used C3B (weight percentage), load (N), and sliding distance (m) as input factors and examined COF, SWR, and weight loss as output features [31–33]. GRA and grey fuzzy analysis were used to improve the abrasive wear findings.

2. Experimental Procedure

2.1. Selection of Materials. Repol H110 MA, as purchased from reliance industries, was chosen as the substance for the matrix because of its melting rate index of 11 g 10 min^{-1} and density of 0.88 g cubic $centimeter^{-1}$. Cloisite 30B was the nanoclay supplied by the southern clay products employed in this investigation (C3B). It was found that EAC has a melting rate of 4 grams per minute and a density of 0.926 grams per cubic $centimeter^{-1}$. C3B dispersion in the PE matrix was improved by the addition of this ingredient.

2.2. Production of Nanocomposites of Polyethylene/C3B/EAC. Polyethylene/Cloisite 30B/Elvaloy AC-3427 NCs were made utilizing a twin-screw extruder and intercalation of the melting process. The parameters for the twin-screw extrusion procedure used to make PE/C3B/EAC nanocomposites were chosen from earlier research [34] and are listed in Table 1.

Figure 1 shows that a twin-screw extruder's temperature may be adjusted at various zones. Injection molding was used to obtain the samples for testing, and the temperature was kept between 170°C and 190°C (from inlet to die area). In the PE matrix, C3B was finely dispersed at 2 wt % and with a high density at 5 wt %, as illustrated in Figures 2(a) and 2(b). The earlier research [35–37] explored the mechanical characteristics of treated materials in terms of their tensile, flexural, impact, and Shore *D* hardness measurements, as well as their thermal properties (DSC, TGA, and dynamic analysis).

3. Tribological Studies

A tribo testing equipment was utilized to conduct tribological investigations based on the ASTM G-99-05 two-body-abrasive wear test. Figure 2 depicts a schematic diagram of the machine. The upper part of a D3 steel disc was covered with 320-grit abrasive paper. A constant sliding velocity of 0.5 m s was used in the wear studies, and input

factors such as C3B weight percentage, load, and sliding distance were also used. According to the abrading direction, the PE/C3B/EAC nanocomposite sample illustrated in Figure 3 is parallel and antiparallel to 320 grit paper. For abrasive wear testing of Polyethylene/Cloisite 30B/Elvaloy AC-3427 NCs, the following assumptions were made: (i) samples with damage were excluded, (ii) there is surface roughness, and (ii) the load is delivered directly to the point of contact.

Experiments were performed to see how much weight was lost. An equation was used to determine the SWR.

$$\text{Specific wear rate}\left(K_s\right) = \frac{m_1 - m_2}{\rho \times N \times S}\,\frac{\text{mm3}}{\text{min}}. \tag{1}$$

In order to calculate the COF, the following equation was used:

$$\text{COF}\,(\mu) = \frac{\text{frictional force}\,(F)}{\text{load}\,(N)}. \tag{2}$$

Samples that had been scratched were examined using a scanning electron microscope.

4. Design of Experiments

Input parameter increases make parameter optimization more challenging. There was a direct correlation between an increase in the number of experiments and an increase in the input parameters. Taguchi techniques employed orthogonal arrays to lessen this complexity. Wear experiments were conducted using parameters such as C3B, load, and sliding distance at 0.5 min/s^{-1} with a constant sliding velocity. For the sake of clarity, the levels and parameters investigated are listed in Table 2. The L′16 orthogonal array was used to construct and conduct the current study's two-body abrasive wear testing. We saw a decrease in body weight, a rise in COF, and a decrease in SWR. Relational analysis in the dark of an efficient method for managing uncertainty and discrete data was presented by grey relational analysis (GRA). Black implies a lack of information, whereas white indicates that there is something there. Between white and black, a grey system contains data. Both the absolute value of the sequences and the connection between the sequences may be measured using the GRA method. Using this method, one may examine the link between sequences with the fewest data points, as well as the number of elements that influence a relationship.

Testing for two-body abrasion was carried out in an orthogonal array. A comparability sequence is a series of sixteen wear trials, each of which was treated as an independent subsystem during GRA. Weight loss, SWR, and COF were all lower under the settings with greater GRG levels. It turns into a single-objective optimization utilizing GRA as a result of this.

4.1. S/N Ratio for Computing Abrasive Wear Characteristics. Weight loss, SWR, and COF were all taken into account while testing the abrasive wear resistance of Polyethylene/Cloisite 30B/Elvaloy AC-3427 NCs. The equation shows the

Table 1: Process parameters for the production of PE/C3B/EAC nanocomposites.

Parameters	Range
Barrel temperature	180°C–230°C
Speed	70 rev/min
Volumetric feed	8 rev/min
Length of cooling	45 cm
Degassing pressure	50 mm Hg

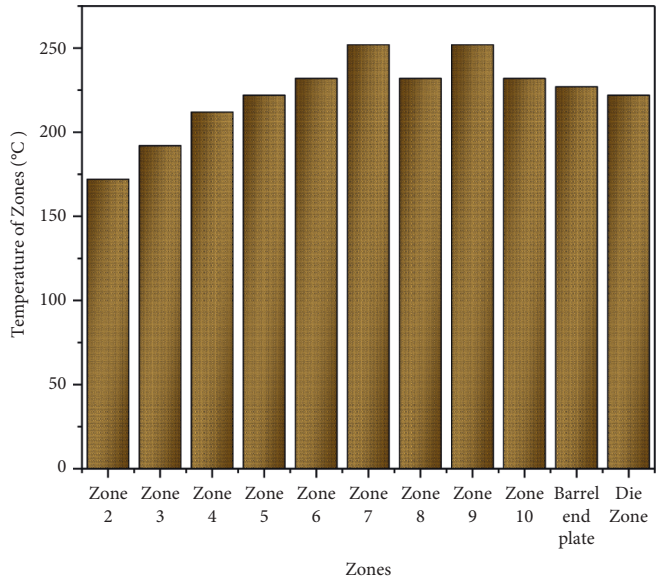

Figure 1: Different temperature zones of TSE.

S/N ratio for attributes where the smaller the value, the better:

$$\frac{S}{\text{N ratio}\ \ (\eta)} = -10\log_{10}\frac{1}{n}\sum_{i=1}^{n}\frac{1}{y_i^2}. \tag{3}$$

4.2. Preprocessing of Data. Data pretreatment was a phrase used to describe the first normalization of experimental data in preparation for GRA. Data preparation is required since each response will have a distinct range and unit. The original sequence was transferred to the equivalent sequence once data preparation was completed. The range of zero to one is used to normalize them for this purpose. Based on the data sequence properties, the preprocessing was done.

It was referred to as "higher-the-better" when the initial value was regarded as infinite and normalized using the following equation:

$$x_i^*\,(k) = \frac{x_i^0\,(k) - \min x_i^0\,(k)}{\max x_i^0\,(k) - \min x_i^0\,(k)}. \tag{4}$$

The normalization of sequence may be done using equation (5) if the lower-the-better qualities are regarded.

$$x_i^*\,(k) = \frac{m\,x_i^0 - x_i^0\,(k)}{m\,x_i^0\,(k) - \text{m}\,x_1^0\,(k)}. \tag{5}$$

As an alternative to this, a normalization of the original sequence using the following would get the desired result.

$$x_i^* (k) = 1 - \frac{\| x_i^0 (k) - x^0 \|}{m\, x_i^0 (k) - x^0}. \quad (6)$$

As an alternative method, the original sequence value may be used and divided by the first digit of the new sequence to arrive at the desired result.

$$x_i^* (k) = \frac{x_i^* (k)}{x_i^0 (1)}. \quad (7)$$

4.3. Calculation of GRG and GRC. GRA is used to assess the relevance of the systems to each other. For the GRA, the sequences employed might be called "grey relational coefficient ξ(k) " which was determined using

$$\xi (k) = \frac{\Delta m + \xi \Delta m}{\Delta oi (k) + \xi \Delta m}. \quad (8)$$

$$\Delta oi - \| x_o^* (k) - x_i^0 (k) \| . \quad (9)$$

$$\Delta \min = \min_{\forall jei} \min_{\forall k} \| x_0^* (k) - x_j^0 (k) \| . \quad (10)$$

$$\Delta m = \max_{\forall jzi} \max_{\forall k} \| x_0^* (k) - x_j^0 (k) \| . \quad (11)$$

Accordingly, GRG was produced by taking the average values of grey the relational coefficient.

$$\gamma_i = \frac{1}{n} \sum_{k=1}^{n} \xi_i (k). \quad (12)$$

Real-time conditions change the relevance of many system variables [30]. Formula (12) can be expanded as follows:

$$\gamma_i = \frac{1}{n} \sum_{k=1}^{n} W_k \xi_i (k). \quad (13)$$

In (13), W_k represents the standardized wt of the element k. Equations (12) and (13) are the same if the values of W_k are the same for all the components. GRG compares the order of the reference sequence to indicate the extent of the effect. Sequences with higher values than the reference sequence will have better GRG values for that sequence, and the reverse is true if the reference sequence has lower values.

4.4. Grey Fuzzy Logic. In order to compute the GRG, three requirements must be met: (i) lower, (ii) higher, and (iii) nominal. To express the problem's ambiguity or lack of knowledge, grey fuzzy logic is used. According to [38–40], when dealing with ambiguity, a set of membership functions is critical. More than one hundred membership functions in the fuzzy set may be used to represent any item in the world that falls inside this range. Fuzzy logic was used to overcome the GRG's flaws.

In the TA part of the fuzzy logic technique, input values are fuzzified before rules are inferred and defuzzified after they have been inferred to provide better results. The comparison of input values with a defuzzification output value yields great prediction accuracy. Fuzzification is the process of applying linguistic factors to a clear number in order to make it fuzzy. In order to answer ambiguous and confusing inquiries, the fuzzy system is utilized, as well as to describe the certainty degree. The fuzzy variables can be assigned membership values using logical techniques. According to prior research, the numerous methods for assigning tasks include inference, rank ordering, intuition, natural networks, angular fuzzy sets, fuzzy statistics, and evolutionary algorithms. A Gaussian, trapezoidal, or triangle membership function is all viable options.

It is possible to derive the rules from the structure presented below by satisfying the following condition.

For linguistic variables, this type of information is known as superficial information. The fuzzy complication operation may be used to determine the membership function of values of fuzzy relations using a variety of ways. Mamdani's complication technique is the implication method of inference used in this study. Applied to fuzzy rule aggregation, it was dubbed max-min inference technique. This is followed by a defuzzification using the maximum membership approach.

Because of the use of fuzzy logic, GRG is more accurate than GRA and has lower levels of uncertainty. As a result, grey fuzzy logic's output is always greater than GRG. As a result, many kinds of applications can benefit from increasing the values of grey fuzzy logic.

Every input and output variable may be accounted for by using ANOVA to determine the proportion of their impact. ANOVA utilized in this investigation will focus on the impact of wear parameters on the SWR and COF output characteristics.

5. Results and Discussion

This part discusses the results of the abrasive wear experiments that were conducted. Grey Relational Analysis and GFL (Grey Fuzzy Logic) are also used to optimize the experimental parameters.

Table 3 shows the sliding distance (m), load (N), and weight loss (weight %) for C3B. Figures 4(a) and 4(b) show the major effect plots for COF and SWR (b). When Cloisite 30B was introduced to Polyethylene matrix NCs at a concentration of 1 weight %, the weight loss was the greatest associated with other concentrations of Cloisite 30B. Cloisite 30B added to the diet resulted in much more weight loss. When C3 B was added to 5 N, the weight loss was found to be lower, and it increased when the load was improved.

Specific wear rate readings were at their highest up to a sliding distance of 150 meters, and as the distance increased, the SWR decreased. In order to build the transfer layer, the PE/C3B/EAC NCs pin had to glide more often over the same surface, which increased the length of time it spent there. SWR values are reduced due to the data of a

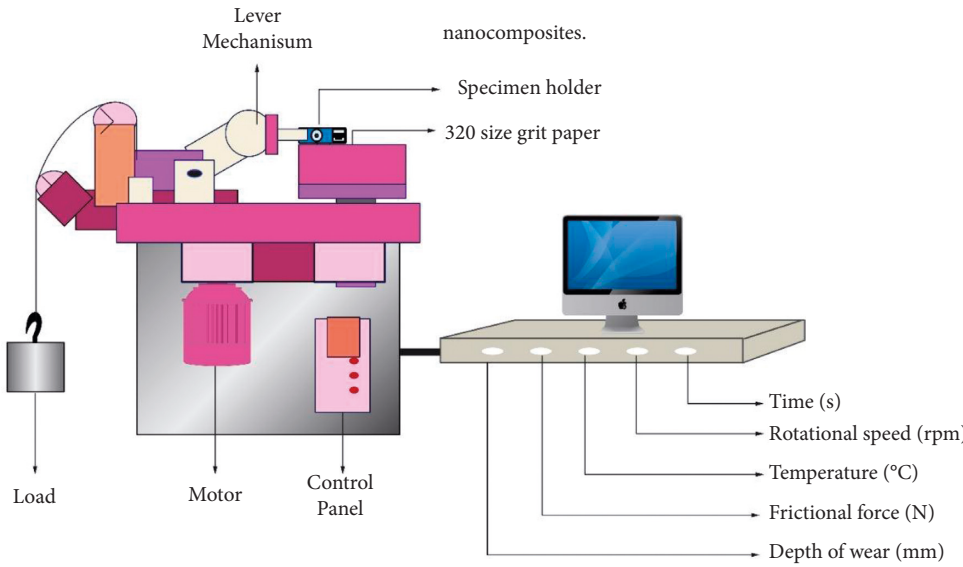

Figure 2: Schematic view of a pin on disc setup.

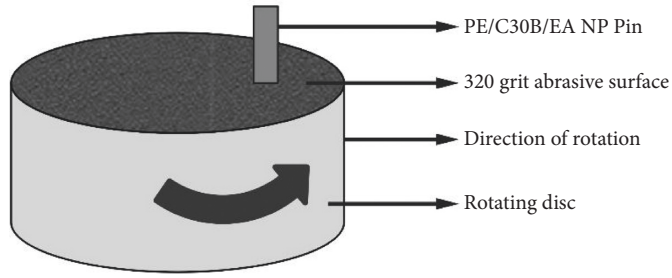

Figure 3: Rotating disc with Polyethylene/C3B/EAC nanocomposite.

Table 2: Control factors and their levels.

Control factors	Levels			
	1	2	3	4
C3B (*wt* %)	2	3	4	5
Load (N)	10	15	20	25
Sliding distance (m)	100	200	300	400

transfer layer on the surface. Specific wear rate values drop when the load is added. Polyethylene/Cloisite 30B/Elvaloy AC-3427 NCs is separated from the surface at 20Nload because of the heat generated at the contact surface. Adding Cloisite 30B at a very low increased the value of specific wear rate, whereas increasing the amount of C3B increased the value of SWR.

Cloisite 30B and Polyethylene composite bear the bulk of the burden. The COF values peaked at 1 weight % of PE/C3B/EAC and dropped as the amount of Cloisite 30B increased to the Polyethylene matrix increased. The rise in thermal stability values at 5 wt % of Polyethylene/Cloisite 30B/Elvaloy AC-3427 NCs, as validated by thermogravimetric testing, is another possible explanation for the lower COF values. When the load was raised, the COF value fell. At the contact zone, there was a temperature shift in the nanocomposite specimen PE/C3B/EAC. The PE/C3B/EAC NC surface partially melts at the 25 N load condition, lubricates the surface, and decreases the coefficient of friction value. A sliding distance of 200 m increases COF readings; however, the values drop as the distance increases. Polyethylene/Cloisite 30B/Elvaloy AC-3427 NCs on the 320-grit surface were clogged when the sliding distance was large, resulting in lower COF values.

5.1. GRA for Abrasive Wear. Analyzing output characteristics, this study used lower-the-better performance characteristics. Polyethylene/Cloisite 30B/Elvaloy AC-3427 NCs SWR, COF, and weight loss as results are shown in Table 4 with grey relationship coefficients of abrasive wear characteristics therein. For each trial, the grey relationship coefficients have a different value. For abrasive wear characteristics, there was a necessity to compute the GFRG.

GRG was determined by averaging the values indicated in Table 4 for each of the input parameters.

With a load of 25 N and an overall sliding distance of 100 meters, the response table determined that the optimal C3B addition was 5 wt %. The computed GRG major effect plot is shown in Figure 5. A GRG value exceeding 0.5 is seen in all three output abrasive wear characteristics.

Table 3: Results for COF, loss of weight, and SWR.

Sl. no.	Cloisite 30B (wt%)	Load (N)	Sliding distance (m)	COF (μ)	Loss of weight (g)	Wear rate (mm^3/Nm)
1	2	10	100	0.302	0.0025	0.007214
2	2	15	200	0.289	0.0089	0.006909
3	2	20	300	0.276	0.0101	0.003501
4	2	25	400	0.252	0.0152	0.002814
5	3	10	200	0.279	0.0049	0.007136
6	3	15	100	0.271	0.0041	0.006142
7	3	20	400	0.249	0.0145	0.003516
8	3	25	300	0.251	0.0114	0.002814
9	4	10	300	0.244	0.0050	0.004679
10	4	15	400	0.239	0.0115	0.004312
11	4	20	100	0.237	0.0107	0.004980
12	4	25	200	0.251	0.0110	0.004012
13	5	10	400	0.247	0.0095	0.004112
14	5	15	300	0.239	0.007	0.003914
15	5	20	200	0.239	0.008	0.003642
16	5	25	100	0.231	0.0039	0.003124

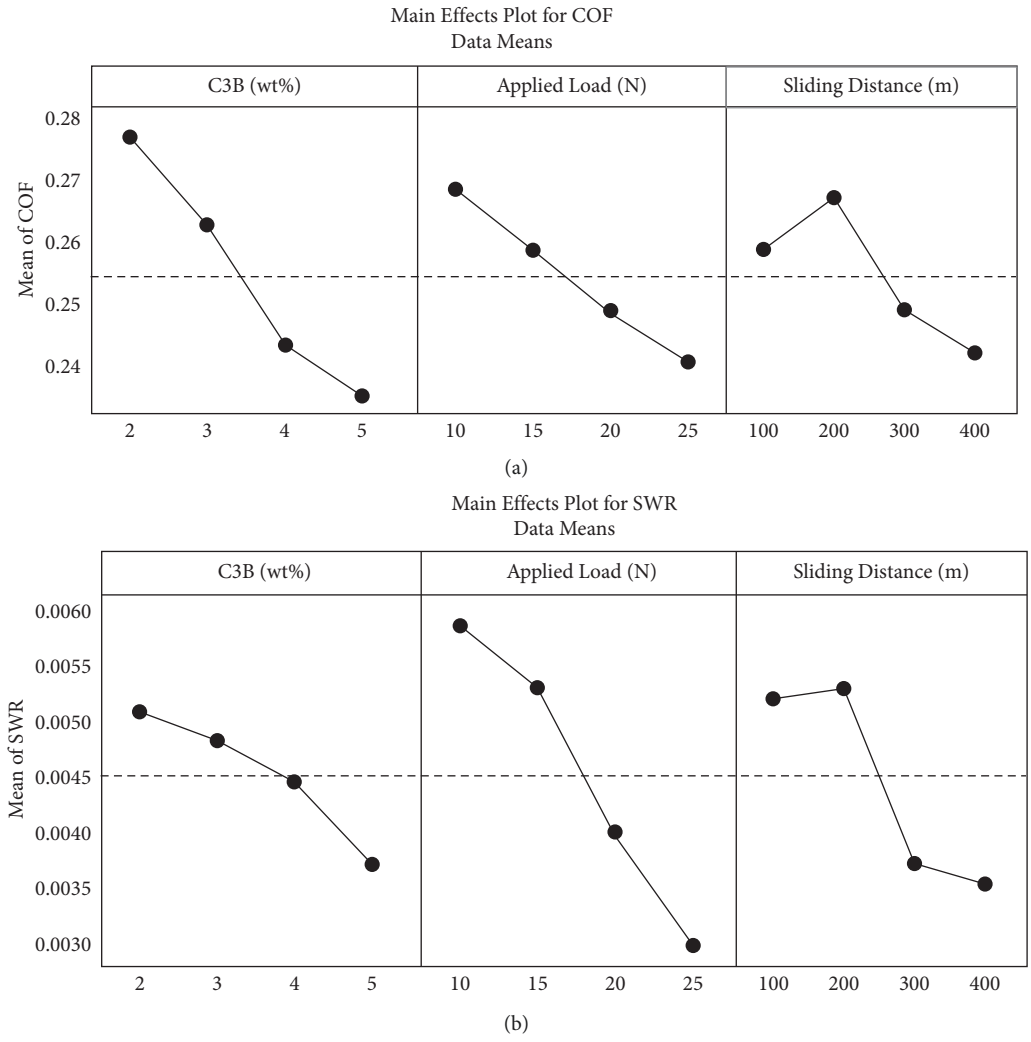

Figure 4: (a) Main effect plots of coefficient of friction. (b) Main effect plots of specific wear rate.

Table 4: The grey relation coefficient and grey relational grade for abrasive wear responses.

Sl. no.	Cloisite 30B (wt%)	Load (N)	Sliding distance (m)	GRC of COF (μ)	GRC for weight loss	GRC for SWR (mm^3/Nm)	GRG	Rank
1	2	10	100	0.329	0.998	0.329	0.542	12
2	2	15	200	0.349	0.481	0.349	0.389	14
3	2	20	300	0.462	0.449	0.741	0.552	16
4	2	25	400	0.679	0.342	1.000	0.669	15
5	3	10	200	0.384	0.719	0.328	0.481	4
6	3	15	100	0.471	0.784	0.401	0.549	11
7	3	20	400	0.609	0.339	0.742	0.574	13
8	3	25	300	0.641	0.421	0.998	0.679	6
9	4	10	300	0.668	0.728	0.531	0.640	2
10	4	15	400	0.739	0.409	0.608	0.580	10
11	4	20	100	0.756	0.442	0.491	0.571	8
12	4	25	200	0.682	0.419	0.642	0.576	7
13	5	10	400	0.712	0.469	0.619	0.612	9
14	5	15	300	0.841	0.519	0.661	0.669	3
15	5	20	200	0.745	0.569	0.728	0.678	5
16	5	25	100	0.998	0.781	0.879	0.881	1

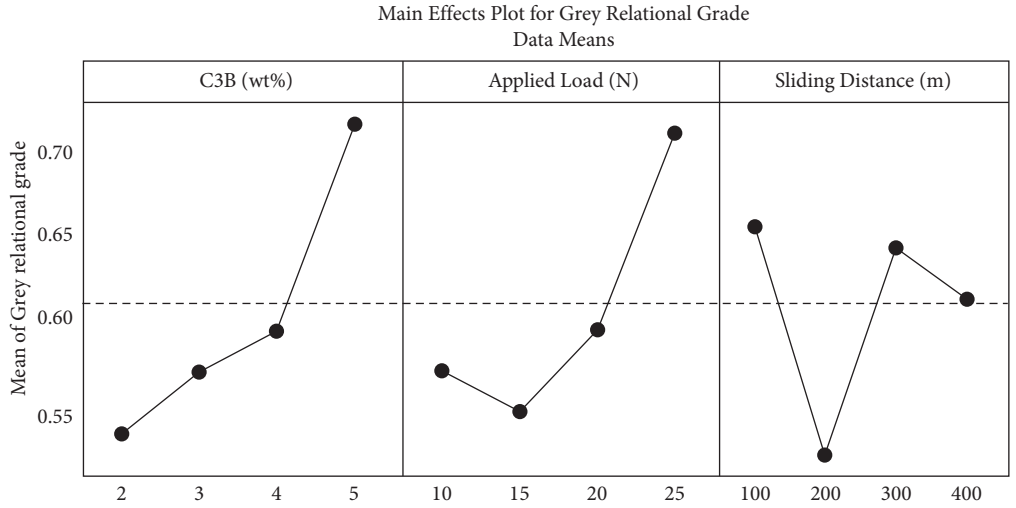

Figure 5: Main effect plots for GRG.

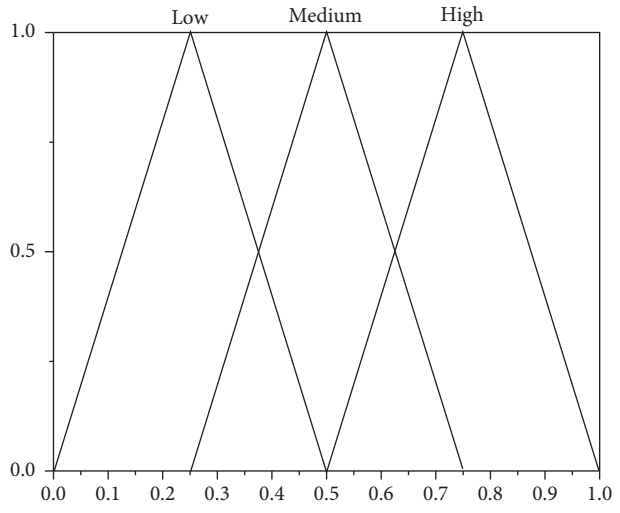

Figure 6: Output characteristics like weight loss, coefficient of friction, and specific wear rate.

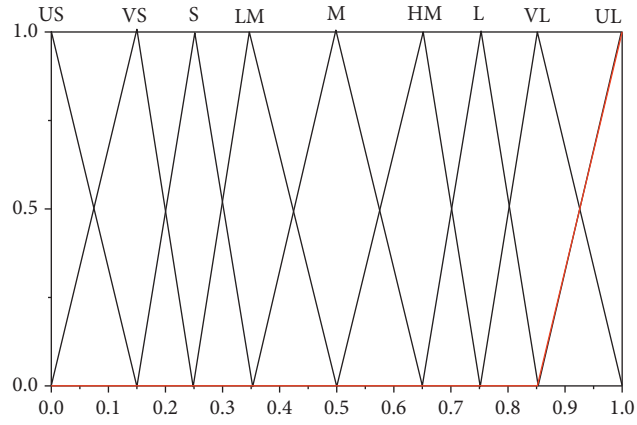

Figure 7: The nine fuzzy subsets for grey fuzzy reasoning grade.

Table 5: The abrasive wear responses at grey fuzzy reasoning grade.

Sl. no.	Cloisite 30B (wt%)	Load (N)	Sliding distance (m)	Grey fuzzy grade	Rank
1	2	10	100	0.571	16
2	2	15	200	0.406	12
3	2	20	300	0.554	4
4	2	25	400	0.679	14
5	3	10	200	0.510	13
6	3	15	100	0.558	15
7	3	20	400	0.569	2
8	3	25	300	0.689	11
9	4	10	300	0.651	8
10	4	15	400	0.602	6
11	4	20	100	0.578	9
12	4	25	200	0.590	10
13	5	10	400	0.612	5
14	5	15	300	0.690	7
15	5	20	200	0.671	1
16	5	25	100	0.897	3

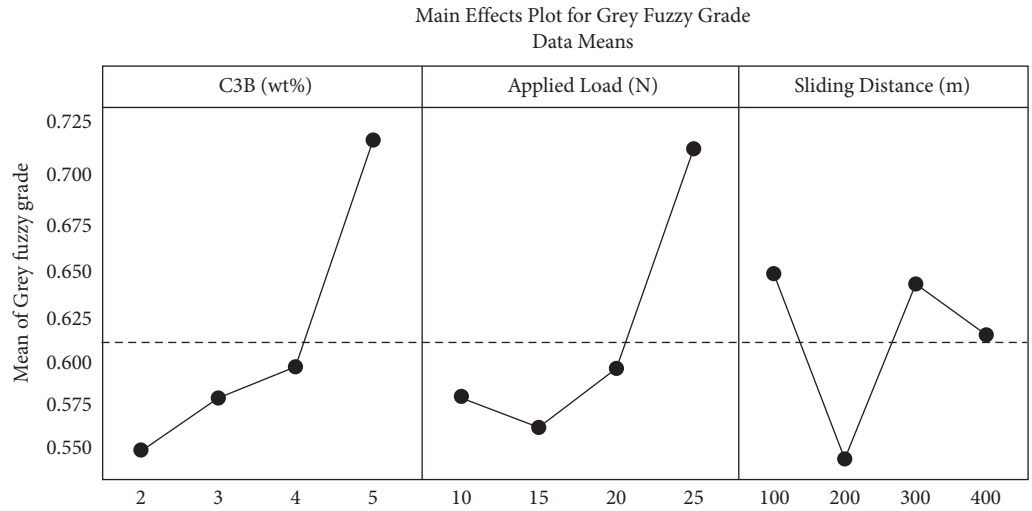

Figure 8: Main effect plots for the grey fuzzy grade.

Table 6: Confirmation test results.

Setting level	Abrasive wear characteristics at an optimum level		
	Parameter	Prediction	Experimental
C3B	10 weight %		
Load	25 Newtons		
Sliding distance	100 meters		
Grey relational grade		0.852	0.895
Grey fuzzy grade		0.858	0.986

When it comes to COF, SWR, and weight loss, the triangle membership function applied in Figure 6 demonstrates the customary nine fuzzy subclasses utilized for the GFRG.

All abrasive wear studies were predicted using the Fuzzy Interface System as shown in Figure 7, which was triggered by establishing a set of guidelines.

Table 5 lists the actual GFR values that were predicted by FIS. Table 4's values were compared to those in Table 5's tables. Compared to GRG, the grey fuzzy reasoning grade went up in terms of performance. The highest grey fuzzy relational grade was recorded in the 16th experiment, which reduced the experiment's uncertainty. Tables 4 and 5 illustrate how much higher the GFRG climbed when associated with GRA. The GRG value has moved to the reference value 1, which reduces fuzziness.

Figure 8 depicts the major impact plot of the abrasive wear features GFRG (Grey fuzzy Reasoning Grade). Cloisite

Table 7: ANOVA table for grey fuzzy grade.

Source	DOF	Adj. SS	Adj. MS	F_{cal}	F_{table}
C3B (wt%)	3	0.07214	0.02861	5.62	3.35
Load (N)	3	0.06187	0.02146	4.75	3.35
Sliding distance (m)	3	0.03214	0.01210	2.57	3.35
Error	6	0.02614	0.00436		
Total	15	0.18960			

03B and load were kept at stage 4, and sliding distance was kept at stage 1 in experiment sixteen, according to the table of results of the grey fuzzy technique.

Once the best circumstances were discovered, the theoretical prevision of GFRG was critical. The equation was used to get the fuzzy reasoning grade (14) where η_{om} is the GFRG mean value and $\overline{\eta_{ol}}$ is the GFRG at the optimal level. Table 6 displays the findings of the confirmation experiment. When compared to GRG, grey fuzzy bond values originated to be greater.

$$\eta_{\text{pre di ctal}} = \eta_{\text{om}} + \sum_{i=1}^{k} \overline{\eta_{ol}} - \eta_{om}, \tag{14}$$

5.2. Analysis of Variance for Grey Fuzzy Grade. Table 7 shows the Analysis of Variance results for the GFG. Each input abrasive wear feature was evaluated using ANOVA to determine the importance of the wear characteristics on the wear characteristics of the output abrasive material. When it came to defining abrasive wear characteristics, C3B addition had the greatest influence, in addition to load and sliding distance.

5.3. Worn Surface Structure. Abrasive wear resistance was improved when Cloisite 30B was introduced at 5% in Polyethylene/C3B/Elvaloy AC-3427 NCs. Abraded surfaces of 5 wt % PE/C3 B/EAC nanocomposites were smooth and less damaged, with indications of PE/C3B/EAC nanocomposites. To remove the matrix from the surface, PE/C3B/EAC nanocomposites must be processed in an agglomerated structure. The abraded surface shows patches of C3B, which enhance the properties' wear resistance. PE/C3B/EAC nanocomposites with a 5-weight % content increased wear resistance significantly due to their improved thermal stability.

The worn surface of Polyethylene/C30B/Elvaloy AC-3427 NCs contains 1 weight %. When C3 B was introduced to the PE matrix at 1 wt %, the abraded surface suffered greater damage than when C3B was applied to the PE matrix at any other concentration. When the PE/C3B/EAC nanocomposites were subjected to ductile fracture, the level of matrix damage was far greater than in any other nanocomposites created. Surface fatigue is the existence of huge, deep grooves on a worn surface. The microploughing and microcracking on the surface of 1 weight % Polyethylene/C30B/Elvaloy AC-3427 NCs were caused by poorer heat stability. The Cloisite 30B element has a proclivity to become free and be eliminated as wear debris where the network of fractures crosses. These nanocomposites were shown to be more susceptible to wear, which may be explained by the reduced ductility of the matrix, which deforms the matrix due to deterioration of the surface at 1weight %. Microcracking and microploughing were the wear processes discovered in this investigation.

6. Conclusion

A twin-screw extruder was utilized to make Polyethylene/Cloisite 30B/Elvaloy AC-3427 NCs. On the basis of abrasion wear testing, the Polyethylene/Cloisite 30B/Elvaloy AC-3427 NCs were defined. Grey Fuzzy and GRA were used to optimize the abrasive wear test results. The following are the findings:

(i) As part of the two-body abrasive wear testing, numerous performance metrics were taken into consideration in order to get the best results. GRA and grey fuzzy were used to optimize the results of two-body abrasive wear testing.

(ii) Grey's fuzzy reasoning grade was boosted by 25 N load, 5 wt % C3B addition, and a sliding distance of 100 m, which was near to the reference value of 0.897 for fuzzy reasoning grade.

(iii) Following sliding distance and load, the quantity of (wt %) addition of C3B was shown to be the most key aspect in inducing the abrasive wear characteristics.

(iv) Abrasive wear test results showed reduced damage to abraded wear surfaces when Cloisite 30B was applied at 5 wt % because more C3B was made public. Microcracking and microploughing were determined to be the abrasive wear mechanisms.

Data Availability

All the available data are included within the manuscript.

Conflicts of Interest

The authors declare that they have no conflicts of interest.

References

[1] D. Jafrey Daniel and K. Panneerselvam, "Modeling of tensile properties, dispersion studies, and hardness evaluation of cloisite 30B in polypropylene with Elvaloy AC 3427 as compatibilizer," *Journal of Composite Materials*, vol. 50, no. 23, pp. 3219–3227, 2016.

[2] A. Singh, S. Datta, S. S. Mahapatra, T. Singha, and G. Majumdar, "Optimization of bead geometry of submerged arc weld using fuzzy based desirability function approach," *Journal of Intelligent Manufacturing*, vol. 24, no. 1, pp. 35–44, 2013.

[3] D. J. Daniel and K. Panneerselvam, "Mechanical and thermal behaviour of polypropylene/cloisite 30B/Elvaloy AC 3427 nanocomposites processed by melt intercalation method," *Transactions of the Indian Institute of Metals*, vol. 70, no. 4, pp. 1131–1138, 2017.

[4] J. C. Rodríguez Hernández, M. Salmerón Sánchez, J. L. Gómez Ribelles, and M. Monleón Pradas, "Polymer-silica nanocomposites prepared by sol-gel technique: nanoindentation and tapping mode AFM studies," *European Polymer Journal*, vol. 43, no. 7, pp. 2775–2783, 2007.

[5] T. V. Sibalija and V. D. Majstorovic, "An integrated approach to optimise parameter design of multi-response processes based on Taguchi method and artificial intelligence," *Journal of Intelligent Manufacturing*, vol. 23, no. 5, pp. 1511–1528, 2012.

[6] H. Baniasadi, A. Ramazani S A, and S. Javan Nikkhah, "Investigation of in situ prepared polypropylene/clay nanocomposites properties and comparing to melt blending method," *Materials & Design*, vol. 31, no. 1, pp. 76–84, 2010.

[7] A. Krishnamoorthy, S. Rajendra Boopathy, K. Palanikumar, and J. Paulo Davim, "Application of grey fuzzy logic for the optimization of drilling parameters for CFRP composites with multiple performance characteristics," *Measurement*, vol. 45, no. 5, pp. 1286–1296, 2012.

[8] D. J. Daniel and K. Panneerselvam, "Manufacturing issues of polypropylene nanocomposite by melt intercalation process," *Materials Today Proceedings*, vol. 4, no. 2, pp. 4032–4041, 2017.

[9] D. J. Daniel and K. Panneerselvam, "Mechanical properties of polypropylene nanocomposites: dispersion studies and modelling," *Transactions of the Indian Institute of Metals*, vol. 71, no. 1, pp. 225–230, 2018.

[10] M. Kato, A. Usuki, and A. Okada, "Synthesis of polypropylene oligomer-clay intercalation compounds," *Journal of Applied Polymer Science*, vol. 66, no. 9, pp. 1781–1785, 1997.

[11] H.-L. Lin, "The use of the Taguchi method with grey relational analysis and a neural network to optimize a novel GMA welding process," *Journal of Intelligent Manufacturing*, vol. 23, no. 5, pp. 1671–1680, 2012.

[12] P. S. Kao and H. Hocheng, "Optimization of electrochemical polishing of stainless steel by grey relational analysis," *Journal of Materials Processing Technology*, vol. 140, no. 1-3, pp. 255–259, 2003.

[13] M. Grzenda, A. Bustillo, and P. Zawistowski, "A soft computing system using intelligent imputation strategies for roughness prediction in deep drilling," *Journal of Intelligent Manufacturing*, vol. 23, no. 5, pp. 1733–1743, 2012.

[14] A. N. Haq, P. Marimuthu, and R. Jeyapaul, "Multi response optimization of machining parameters of drilling Al/SiC metal matrix composite using grey relational analysis in the Taguchi method," *International Journal of Advanced Manufacturing Technology*, vol. 37, no. 3–4, pp. 250–255, 2008.

[15] C. L. Lin, J. L. Lin, and T. C. Ko, "Optimisation of the EDM process based on the orthogonal array with fuzzy logic and grey relational analysis method," *International Journal of Advanced Manufacturing Technology*, vol. 19, no. 4, pp. 271–277, 2002.

[16] Y.-C. Lin and H.-S. Lee, "Optimization of machining parameters using magnetic-force-assisted EDM based on gray relational analysis," *International Journal of Advanced Manufacturing Technology*, vol. 42, no. 11–12, pp. 1052–1064, 2009.

[17] S. Datta, A. Bandyopadhyay, and P. K. Pal, "Grey-based taguchi method for optimization of bead geometry in submerged arc bead-on-plate welding," *International Journal of Advanced Manufacturing Technology*, vol. 39, no. 11–12, pp. 1136–1143, 2008.

[18] S. Kumar and R. Singh, "Optimization of process parameters of metal inert gas welding with preheating on AISI 1018 mild steel using grey based Taguchi method," *Measurement*, vol. 148, Article ID 106924, 2019.

[19] R. Nalini, S. Nagarajan, and B. S. R. Reddy, "Polypropylene-blended organoclay nanocomposites - preparation, characterisation and properties," *Journal of Experimental Nanoscience*, vol. 8, no. 4, pp. 480–492, 2013.

[20] N. Tosun, "Determination of optimum parameters for multi-performance characteristics in drilling by using grey relational analysis," *International Journal of Advanced Manufacturing Technology*, vol. 28, no. 5-6, pp. 450–455, 2006.

[21] S.-H. Lim, A. Dasari, G. T. Wang et al., "Impact fracture behaviour of nylon 6-based ternary nanocomposites," *Composites Part B: Engineering*, vol. 41, no. 1, pp. 67–75, 2010.

[22] A. C. Chinellato, S. E. Vidotti, G.-H. Hu, and L. A. Pessan, "Compatibilizing effect of acrylic acid modified polypropylene on the morphology and permeability properties of polypropylene/organoclay nanocomposites," *Composites Science and Technology*, vol. 70, no. 3, pp. 458–465, 2010.

[23] W. Lertwimolnun and B. Vergnes, "Influence of compatibilizer and processing conditions on the dispersion of nanoclay in a polypropylene matrix," *Polymer*, vol. 46, no. 10, pp. 3462–3471, 2005.

[24] R. Ranjith, P. K. Giridharan, J. Devaraj, and V. Bharath, "Influence of titanium-coated (B4Cp+ SiCp) particles on sulphide stress corrosion and wear behaviour of AA7050 hybrid composites (for MLG link)," *Journal of the Australian Ceramic Society*, vol. 53, no. 2, pp. 1017–1025, 2017.

[25] S. Zhang, T. R. Hull, A. R. Horrocks et al., "Thermal degradation analysis and XRD characterisation of fibre-forming synthetic polypropylene containing nanoclay," *Polymer Degradation and Stability*, vol. 92, no. 4, pp. 727–732, 2007.

[26] R. Ranjith, P. K. Giridharan, C. Velmurugan, and C. Chinnusamy, "Formation of lubricated tribo layer, grain boundary precipitates, and white spots on titanium-coated graphite–reinforced hybrid composites," *Journal of the Australian Ceramic Society*, vol. 55, no. 3, pp. 645–655, 2019.

[27] R. Ranjith and P. K. Giridharan, "Experimental investigation of surface hardness and dry sliding wear behavior of AA7050/B 4 C p," *High Temperature Material Processes: An International Quarterly of High-Technology Plasma Processes*, vol. 19, no. 3-4, pp. 291–305, 2015.

[28] K. Palanikumar, "Experimental investigation and optimisation in drilling of GFRP composites," *Measurement*, vol. 44, no. 10, pp. 2138–2148, 2011.

[29] R. Ranjith and P. K. Giridharan, "Influence of high temperature on surface hardness of AA7050 hybrid composites," *Journal of Materials and Environmental Science*, vol. 8, pp. 1168–1172, 2017.

[30] L. A. Zadeh, "Fuzzy sets," *Information and Control*, vol. 8, no. 3, pp. 338–353, 1965.

[31] R. Ranjith, P. K. Giridharan, J. Devaraj, and S. Balamurugan, "Frictional behavior of the aa7050/b 4 c p aluminum

composites," *Composites: Mechanics, Computations, Applications, An International Journal*, vol. 9, no. 1, pp. 17–25, 2018.

[32] K.-T. Chiang, N.-M. Liu, and C.-C. Chou, "Machining parameters optimization on the die casting process of magnesium alloy using the grey-based fuzzy algorithm," *International Journal of Advanced Manufacturing Technology*, vol. 38, no. 3–4, pp. 229–237, 2008.

[33] D. D. Jafrey and K. Panneerselvam, "Study on tensile strength, impact strength and analytical model for heat generation in friction vibration joining of polymeric nanocomposite joints," *Polymer Engineering & Science*, vol. 57, no. 5, pp. 495–504, 2017.

[34] S. Shokoohi, A. Arefazar, and G. Naderi, "Compatibilized Polypropylene/Ethylene-Propylene-Diene-Monomer/Polyamide6 ternary blends: effect of twin screw extruder processing parameters," *Materials & Design*, vol. 32, no. 3, pp. 1697–1703, 2011.

[35] H. M. Akil, M. F. A. Rasyid, and J. Sharif, "Effect of compatibilizer on properties of polypropylene layered silicate nanocomposite," *Procedia Chemistry*, vol. 4, pp. 65–72, 2012.

[36] V. Kumar, J. Ramkumar, S. Aravindan, S. K. Malhotra, K. Vijai, and M. Shukla, "Fabricationand characterization of ABS nano composite reinforced by nano sized alumina particulates," *Int. J. Plast. Technol*, vol. 13, no. 2, pp. 133–149, 2009.

[37] B.-P. Chang, H. M. Akil, and R. B. M. Nasir, "Comparative study of micro- and nano-ZnO reinforced UHMWPE composites under dry sliding wear," *Wear*, vol. 297, no. 1–2, pp. 1120–1127, 2013.

[38] K. R. Sumesh, V. Kavimani, G. Rajeshkumar, P. Ravikumar, and S. Indran, "An investigation into the mechanical and wear characteristics of hybrid composites: influence of different types and content of biodegradable reinforcements," *Journal of Natural Fibers*, vol. 17, pp. 1–13, 2020.

[39] H. S. Lu, C. K. Chang, N. C. Hwang, and C. T. Chung, "Grey relational analysis coupled with principal component analysis for optimization design of the cutting parameters in high-speed end milling," *Journal of Materials Processing Technology*, vol. 209, no. 8, pp. 3808–3817, 2009.

[40] S. Keerthiveettil Ramakrishnan, K. Vijayananth, G. Pudhupalayam Muthukutti, P. Spatenka, A. Arivendan, and S. P. Ganesan, "The effect of various composite and operating parameters in wear properties of epoxy-based natural fiber composites," *Journal of Material Cycles and Waste Management*, vol. 24, no. 2, pp. 667–679, 2022.